Experimental and Numerical Study of Moisture-induced Stress Formation in Hexagonal Glulam Using X-ray Computed Tomography and Finite-element Analysis

Rongrong Li,[a] Pingxiang Cao,[a] Wei Xu,[a] Mats Ekevad,[b] and Xiaodong (Alice) Wang [c]

Hexagonal glue-laminated timber with large cross-sections, made from small diameter logs, was studied. Effects of relative humidity variations on the moisture-induced stresses were investigated to evaluate how the prediction model compared to a real outcome. The test samples were exposed to an environment with relative humidity variations from 80% to 30%. The moisture content inside the samples was measured *via* X-ray computed tomography scanning. A moisture transport and a hygro-mechanical finite element simulation model was used for the prediction of moisture content and resulting stress distribution. The results from both the test and simulation showed that the moisture content in the edge angles of the samples dropped rapidly due to a large moisture diffusion rate. The moisture gradient was generated *via* a different moisture transfer rate at the inner and external parts of the samples. The maximum stress perpendicular to the grain in the simulation was 8 MPa and was located at the surface near the corners. This stress peak caused cracking according to the model, which was also seen in the test samples. The results for the measured moisture content agreed with the simulated results and this indicated that the moisture transfer model was adequate for simulation.

Keywords: Glulam; X-ray computed tomography; Finite element model; Climate variations; Moisture-induced stress

Contact information: a: Co-Innovation Center of Efficient Processing and Utilization of Forest Resources, Nanjing Forestry University, Nanjing, China 210037; b: Division of Wood Science and Engineering, Luleå University of Technology, Skellefteå, Sweden SE-93187; c: Department of Wood and Forest Sciences, Laval University, Pavillon Kruger, Quebec, Canada G1V 0A6;
** Corresponding author: lirongrong@njfu.edu.cn*

INTRODUCTION

Glued laminated timber (glulam) is made by joining a number of wood laminates *via* a gluing process (Li *et al.* 2015). The use of small dimension lumber to manufacture large wooden structural members with a desired shape and size is a distinct advantage of glulam. This allows glulam to have a high utilization of the raw wood materials, as well as additional value (Anshari *et al.* 2012). For sustainable constructions, glulam is used as beams and columns in buildings or structures, as well as carrying mechanical loads, but it is also affected by climate variations in their surrounding environment (Mirzaei *et al.* 2017). Climate variations in the environment result in moisture and temperature gradients in wood, primarily forming perpendicular to the grain (Zhan *et al.* 2018a,b). These gradients induce stress in the wood and may even cause cracking in the glue-laminated timber, which affects the safety and performance of the sustainable wooden structures in service. Climate variations include changes in relative humidity (RH) and temperature

variations. Unless the change in humidity is slow, considerable moisture gradients will form, which generates stresses primarily perpendicular to the grain. When the moisture induced stresses (MIS) become higher than the tensile strength perpendicular to the grain, cracks will form in the wood material. Crack formation and propagation decreases the load-bearing capacity of the wood material and will affect the stability and safety of the timber structures. Therefore, it is important to investigate the effects of variations in climate on the performance of glulam.

Published articles indicate that many parameters affect MIS, including the type of climate, the size of the timber cross-section, and the type of protective coating (Jonsson 2004; Ekevad *et al.* 2011; Ekevad and Axelsson 2012; Knorz *et al.* 2016; Sepulveda-Villarroel *et al.* 2016). Angst and Malo (2013) studied the moisture distribution and development of MIS over time in various glulam cross-sections during wetting *via* numerical simulations. The results showed that the local stresses were significantly larger than the average stresses, and moreover they were strongly dependent on the geometrical configuration of the glulam laminates (Angst and Malo 2013). Fragiacomo *et al*. investigated the influence of the main parameters (such as the type of climate, the size of the timber cross-section, and the type of protective coating) on MIS. In their work, the moisture distribution and the corresponding stress distribution was calculated *via* a diffusion (Fickian) moisture transfer model and a mechanical model, respectively, for the time dependent behavior of wood. The results showed that a northern European climate had higher moisture gradients and thus a higher MIS when compared to a southern European climate; furthermore, that the MIS could be effectively reduced by coatings, which also effectively reduced the probability of cracks (Fragiacomo *et al.* 2011). Svensson *et al.* (2011) also used a diffusion (Fickian) moisture transfer model to predict the moisture state of timber members in varying climates, where the effects of a continuously varying humidity on timber members were characterized. The results indicated that the moisture fluctuation on the surface of a timber member was strongly dependent upon the amplitude of the RH variations but was not affected by the average value of the harmonic RH variations too much, and the MIS was also influenced by the initial moisture state of the timber. Zhu *et al*. developed a three-dimensional (3D) finite element (FE) procedure to investigate the hygro-thermal stress in glulam beams. The modelling was successful in describing the moisture content (MC), temperature, and stress distributions in glulam beams (Zhou *et al.* 2010).

The present study focused on hexagonal glulam with large cross-section made from small-diameter Chinese fir (*Cunninghamia lanceolata*) logs. To achieve high additional value and develop the application area, the small diameter logs were selected to manufacture glulam expected to be used in wooden structures. This glulam material is built from hexagonally shaped cross-sections from small-diameter logs in full and half format that are glued together, as shown in Fig. 1a and Fig. 2. The resulting hexagonal glulam material can be used as beams and pillars with a large cross-sectional area. However, because it has been reported earlier that the MIS are strongly affected by the geometrical configuration of the glulam, a more advanced hexagonal shaped glulam is studied in this work. Moreover, the small-diameter logs, used for the glulam in this study, have a lower mechanical strength and shape stability than the larger diameter logs, which increased the probability of cracking. The aim of the study is to investigate the MC distribution and evaluate the MIS in hexagonal glulam *via* X-ray computed tomography (CT-scanning) and a hygro-mechanical finite-element simulation model.

EXPERIMENTAL

Materials

The species of wood used for the hexagonal glulam was Chinese fir (*Cunninghamia lanceolata*), which was harvested in Jiangxi, China. The adhesive used for manufacturing glulam was polyurethane adhesive (Dynea, Shanghai, China). The moisture distribution of the hexagonal glulam was measured during drying from 80% RH to 30% RH in a CT scanner (SIMENS, Munich, Germany). The MC and the MIS were also simulated using a FE model implemented with ABAQUS software (DASSAULT SIMULIA, ABAQUS/ CAE 2016, Rhode Island, USA). The calculated results of the moisture distribution were compared with the results of the experiments to verify the accuracy of the FE modeling. The CT-scanning also detected cracks that formed in the glulam. The temperature of the test environment was constant with the value of 20 ℃ in this study.

Methods

MC measurements using CT-scanning

In the present study, the initial MC and temperature of the wood samples were assumed to be uniformly distributed and in equilibrium with its environment. When the RH of the surrounding environment changed, the MC in the glulam began to change, thus forming MC gradients. The exchange of moisture did not stop until a new equilibrium was reached. Ten samples with lengths of 150 mm were prepared (shown in Fig. 1a) and seasoned in a climate chamber with a RH and temperature of 80% and 20 °C, respectively, until the moisture distribution of the samples was stable.

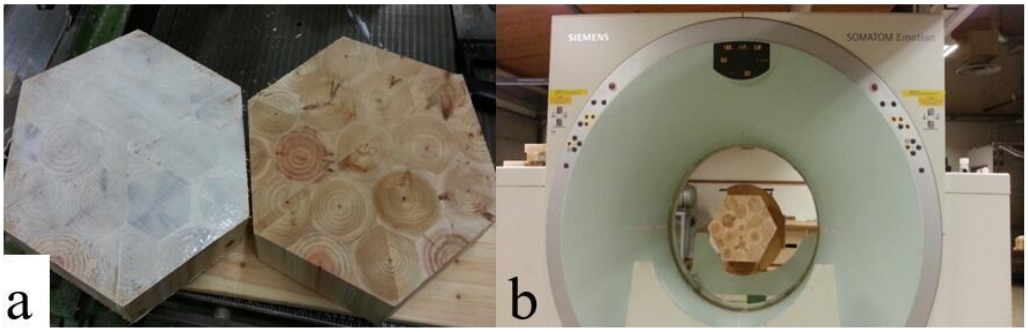

Fig. 1. Samples and experimental setup in the CT scanner

The dimensions of the samples are shown in Fig. 2. Due to the short length of the samples, the cross-sectional surfaces were sealed by a silicone adhesive (ESSVE, Kista, Sweden) to prevent moisture transfer in the direction of the fibers. This left only the hexagonal side surfaces exposed to the air. The measurements of the MC were taken using a SIEMENS CT scanner (SIMENS, Munich, Germany) (shown in Fig. 1b). The contrast in CT images was given by the density differences, which was in turn related to the MC of the wood. Using a CT for the measurement of MC in wood is an indirect method, described by Vaziri *et al*. (2011). Basically, the density differences were mapped and located within the material. The density for the volume of each element was normalized to the density of water (calculated absorption coefficient for water), and in relation to the green wood density and the oven-dried density, which gave information about the MC distribution in

the material. For drying, the samples were exposed to 30% RH after first being conditioned at 80% RH, as described above. The RH values selected were according to a typical climate condition in northern China. There were 11 uniformly distributed measurement positions for the MCs in the samples, located along a diagonal line, as shown in Fig. 2.

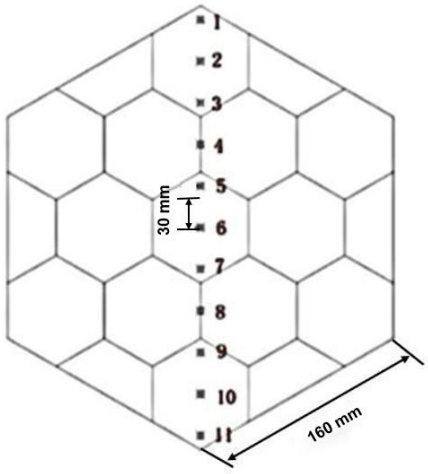

Fig. 2. Measurement positions for MCs

FE-modelling for moisture transfer

In this research, the cross section of hexagonal glulam was sealed to prevent moisture transfer. Thus, the moisture transfer is able to take place only in the radial and tangential directions. The moisture transport model was adapted from Angst and Malo (Angst and Malo 2010, 2012), where a two-dimensional (2D) numerical simulation of the MIS was performed. In a one-dimensional formulation, the moisture transfer in hexagonal glulam can be expressed as Eq. 1,

$$\frac{\partial u}{\partial t} = \frac{\partial}{\partial x}\left(D\,\frac{\partial u}{\partial x}\right) \quad (1)$$

where u is the moisture content (%; the weight of water in a wood sample/the oven-dry weight of a wood sample) and D (m^2s^{-1}) is the corresponding diffusion coefficient. For simplicity reasons, the diffusion coefficient D was assumed equal in radial and tangential direction with the value of $D = 7 \times 10^{-7}\ m^2 s^{-1}$ (Fortino *et al*. 2009).

The moisture flow from the glulam surface to air, termed as the surface emission, was expressed by Eq. 2 (Danvind and Ekevad 2006; Angst and Malo 2010),

$$\left(D\,\frac{\partial u}{\partial x}\right) = S\left(u_{eq} - u_{surf}\right) \quad (2)$$

where S ($m{\cdot}s^{-1}$) is the surface emission factor with a value of $S = 2.5 \times 10^{-8}\ m \cdot s^{-1}$, which takes into account the moisture transfer resistance at the boundary surface, u_{eq} (%) and u_{surf} (%) are the equilibrium MC and the actual surface MC, respectively. The moisture flow was driven by the difference between u_{surf} and u_{eq}. According to the set environmental conditions, the values of u_{surf} and u_{eq} were 0.047 and 0.17, respectively. For the moisture transfer analyses in this simulation, a 2D model extracted from the 3D model and the DC3D20 20-node quadratic heat transfer brick of ABAQUS was selected. The initial condition of a uniform 17% MC was assumed for all hexagonal glulam cross-sections.

FE-modelling for MIS

In the second stage, the hygro-mechanical behavior was modeled by applying a 2D orthotropic material model. The model was used for the calculation of MIS resulting from MC variations. Generally, the total strain rate vector $\dot{\varepsilon}$ was calculated with Eq. 3,

$$\dot{\varepsilon} = \dot{\varepsilon_e} + \dot{\varepsilon_s} + \dot{\varepsilon_v} \quad (3)$$

where $\dot{\varepsilon}$ is the total strain rate (MPa^{-1}), $\dot{\varepsilon_e} = C \cdot \dot{\sigma}$ is the elastic strain rate vector (MPa^{-1}), and *C* is the compliance matrix, shown in Eq. 4,

$$C = \begin{bmatrix} \frac{1}{E_R} & \frac{-v_{TR}}{E_T} & 0 \\ \frac{-v_{RT}}{E_R} & \frac{1}{E_T} & 0 \\ 0 & 0 & \frac{1}{G_{RT}} \end{bmatrix} \quad (4)$$

The characters in Eq. 4, *E* (MPa), *G* (MPa), and *v*, denote the moduli of elasticity, the shear moduli, and Poisson's ratios, respectively, while *R* and *T* denote the radial and tangential directions of wood, respectively. The linear shrinkage-swelling strain rate is expressed as Eq. 5,

$$\dot{\varepsilon_s} = \alpha \cdot \dot{u} \quad (5)$$

where $\dot{u}$ is the rate of the MC variation in glulam and α is the hygro-expansion coefficient vector, shown in Eq. 6,

$$\alpha = [\alpha_R \quad \alpha_T \quad 0]^T \quad (6)$$

where α_R and α_T are hygro-expansion coefficient vector in radial and tangential directions of wood, respectively.

The viscoelastic strain rate vector is shown by $\dot{\varepsilon_v} = V \cdot \dot{\sigma}$ and *V* is the compliance matrix, shown in Eq. 7,

$$V = \begin{bmatrix} \frac{1}{E_R} & \frac{-v_{TR}}{E_T} & 0 \\ \frac{-v_{RT}}{E_R} & \frac{1}{E_T} & 0 \\ 0 & 0 & \frac{1}{G_{RT}} \end{bmatrix} \quad (7)$$

In Eq. 3, the time-dependent creep was neglected in the strain-rate formulation because of the small effect of the time-dependent creep at low MCs compared to the mechano-sorptive creep, as reported by Angst and Malo (Toratti and Svensson 2000; Virta *et al.* 2006).

The species of wood used for the hexagonal glulam was Chinese fir (*Cunninghamia lanceolata*) with a density of 316 kg/m^3 and with 12% MC. The input parameters for the FE simulations were taken from published literature (Table 1) (Danvind and Ekevad 2006; Zhou *et al.* 2010; Fragiacomo *et al.* 2011; Yu *et al.* 2011). For the ABAQUS FE modeling, the mesh used had 9120 type C3D20R elements.

Table 1. Parameters for FE simulations

Model	Parameters	Parameters Sources
Hygro-expansion Coefficients	α_R = 0.13, α_T = 0.27	Fitting (Zhou *et al.* 2010; Yu *et al.* 2011)
Stiffness Parameters	E_R = 752 MPa, E_T = 470 MPa v_{RT} = 0.470, G_{RT} = 67 MPa v_{TR} = 0.294	Fitting (Yu *et al.* 2011)
Viscoelastic Parameters	E_R = 404 MPa, E_T = 244 MPa v_{RT} = 0.87, G_{RT} = 67 MPa v_{TR} = 0.92	Fitting (Jiang *et al.* 2016)

RESULTS AND DISCUSSION

Moisture Distribution

The MC values from the experiments and numerical simulations are shown in Fig. 3. The MC in the immediate vicinity of the surface was more affected by the varying RH, whereas the interior part was less influenced, which was reasonable. The MC near the edge-angle corners of the hexagon dropped rapidly due to the large moisture diffusion surface at the corners. The MC gradients were initially large and became lower with time and the MC also decreased when the distance from the surface increased.

Moisture transfer almost stopped after 8 weeks, and the MC distribution became apparently stable, even though a small moisture gradient still existed. The MC distributions had good agreement between the experimental results and the numerical simulation results.

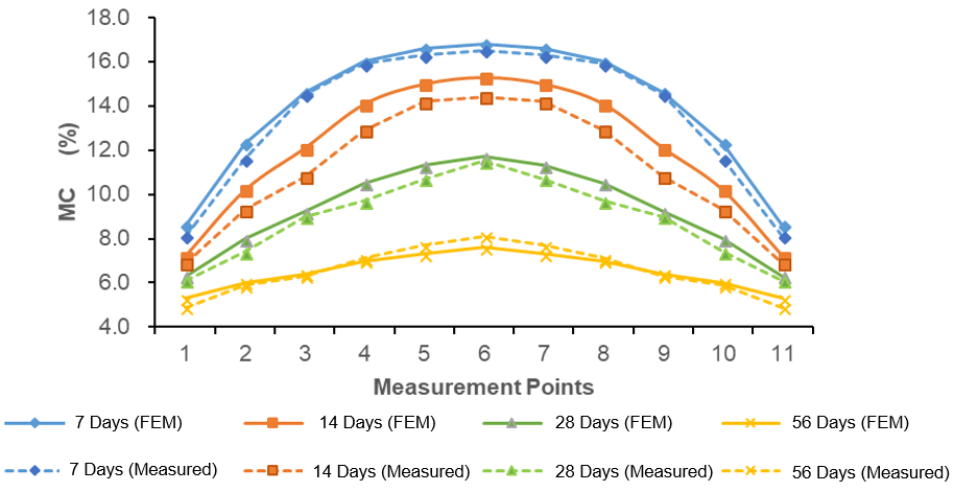

Fig. 3. Moisture content distribution after 7, 14, 28, and 56 days of drying (from 80% RH to 30% RH)

MIS in the Wood

The MIS found perpendicular to the grain, during the 56 days of drying process (80% RH to 30% RH), was calculated using the FE software, ABAQUS. The maximum principal stresses were evaluated at different time steps, as shown in Fig. 4, an example of a stress distribution at one-time step. The outermost parts of the cross-section exhibited relatively fast moisture changes, whereas in the central part, deviations from the initial

equilibrium state required more time. The internal MIS was generally compressed in the center and tensile near the boundaries of the cross-section. In the outermost parts, the maximum tensile stresses were up to 8 MPa (the maximum principal stress calculated using ABAQUS), which was approximately 4 times the stress in the center. Cracks would then most probably form on the outer part of the cross-section, near the corners, when the maximum tensile stress became higher than the tensile strength perpendicular to the wood grain. Figure 5 shows that from the experimental CT scanning, some cracks were generated by high MIS near the corners of the cross-section. This indicated that the FE model was adequate and predicted the positions for the highest MIS. These results are important for guiding the practical production and design process for hexagonal glulam. For this type of glulam, some coating protection is essential to prevent the moisture transfer, thus improving the performance of the glulam.

Further studies are required to fully study and understand this complex and challenging topic; more elaborate models to achieve realistic moisture distributions and MIS in hexagonal glulam are essential. Both the RH and the temperature variations should be assumed to simulate the varying climate. Non-linear mechanical behavior could be used to simulate realistic cracking behavior and thereby give opportunities to improve the design and performance of sustainable building construction elements.

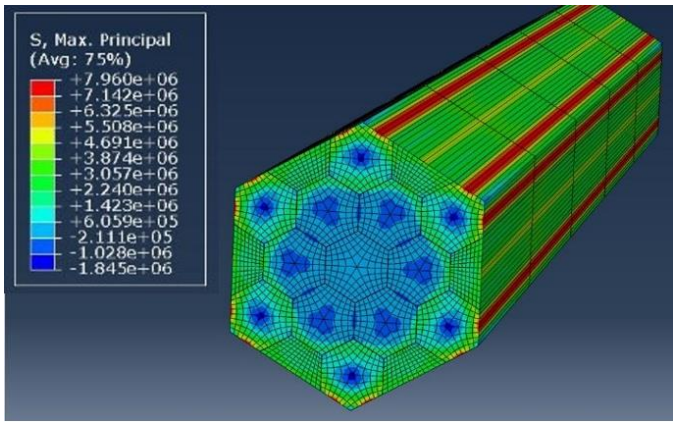

Fig. 4. MIS distribution in glulam

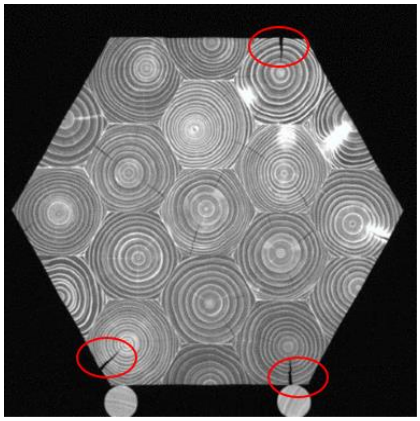

Fig. 5. Cracks in samples

CONCLUSIONS

1. The measured results of the MC in the hexagonal glulam were in good agreement with the results from the numerical FE simulations. The MIS was concentrated near the edge corner areas. The maximum principal tensile stress from the simulations was 8 MPa, and the experimental results showed that this led to small cracks near the corners of the hexagonal glulam, even without external load, just from drying-induced stress. Therefore, the MIS of a large cross-section glulam induced cracks that reduced the load-bearing capacity and affected the failure behavior of the glulam wooden component.
2. The model of the moisture transfer and the mechanical model of wood used in this paper were effective to predict the MC distribution and the MIS in hexagonal glulam.

The results of this study are important to guide the design and manufacturing of hexagonal glulam.

ACKNOWLEDGMENTS

The authors are grateful for the support from the Natural Science Foundation of Jiangsu Higher Education Institutions (18KJB220008), the China Postdoctoral Science Foundation funded project (2017M610778), and the Nanjing Forestry University Youth Science and Technology Innovation Fund (CX2017009).

REFERENCES CITED

Angst, V., and Malo, K. A. (2010). "Moisture induced stresses perpendicular to the grain in glulam: Review and evaluation of the relative importance of models and parameters," *Holzforschung* 64(5), 609-617. DOI: 10.1515/hf.2010.089

Angst, V., and Malo, K. A. (2012). "The effect of climate variations on glulam – An experimental study," *European Journal of Wood and Wood Products* 70(5), 603-613. DOI: 10.1007/s00107-012-0594-y

Angst, V., and Malo, K. A. (2013). "Moisture-induced stresses in glulam cross sections during wetting exposures," *Wood Science and Technology* 47(2), 227-241. DOI: 10.1007/s00226-012-0493-8

Anshari, B., Guan, Z. W., Kitamori, A., Jung, K., and Komatsu, K. (2012). "Structural behaviour of glued laminated timber beams pre-stressed by compressed wood," *Construction and Building Materials* 29, 24-32. DOI: 10.1016/j.conbuildmat.2011.10.002

Danvind, J., and Ekevad, M. (2006). "Local water vapor diffusion coefficient when drying Norway spruce sapwood," *Journal of Wood Science* 52(3), 195-201. DOI: 10.1007/s10086-005-0753-4

Ekevad, M., and Axelsson, A. (2012). "Variation of modulus of elasticity in the tangential direction with moisture content and temperature for norway spruce (*Picea Abies*)," *BioResources* 7(4), 4730-4743. DOI: 10.15376/biores.7.4.4730-4743

Ekevad, M., Lundgren, N., and Flodin, J. (2011). "Drying shrinkage of sawn timber of Norway spruce (*Picea abies*): Industrial measurements and finite element simulations," *Wood Material Science & Engineering* 6(1-2), 41-48. DOI: 10.1080/17480272.2010.523121

Fortino, S., Mirianon, F., and Toratti, T. (2009). "A 3D moisture-stress FEM analysis for time dependent problems in timber structures," *Mechanics of Time-Dependent Materials* 13(4), 333-356. DOI: 10.1007/s11043-009-9103-z

Fragiacomo, M., Fortino, S., Tononi, D., Usardi, I., and Toratti, T. (2011). "Moisture-induced stresses perpendicular to grain in cross-sections of timber members exposed to different climates," *Engineering Structures* 33(11), 3071-3078. DOI: 10.1016/j.engstruct.2011.06.018

Jiang, J., Erik Valentine, B., Lu, J., and Niemz, P. (2016). "Time dependence of the orthotropic compression Young's moduli and Poisson's ratios of Chinese fir wood," *Holzforschung* 70(11), 1093-1101. DOI: 10.1515/hf-2016-0001

Jonsson, J. (2004). "Internal stresses in the cross-grain direction in glulam induced by climate variations," *Holzforschung* 58(2), 154-159. DOI: 10.1515/hf.2004.023

Knorz, M., Niemz, P., and Van de Kuilen, J.-W. (2016). "Measurement of moisture-related strain in bonded ash depending on adhesive type and glueline thickness," *Holzforschung* 70(2), 145-155. DOI: 10.1515/hf-2014-0324

Li, Z., Zhang, J., and Sun, Y. (2015). "Influence of accelerated aging tests on properties of glued-laminated timber," *Journal of Forestry Engineering* 29(1), 94-97. DOI: 10.13360/j.issn.1000-8101.2015.01.027

Mirzaei, G., Mohebby, B., and Ebrahimi, G. (2017). "Glulam beam made from hydrothermally treated poplar wood with reduced moisture induced stresses," *Construction and Building Materials* 135, 386-393. DOI: 10.1016/j.conbuildmat.2016.12.178

Sepulveda-Villarroel, V., Perez-Pena, N., Salinas-Lira, C., Salvo-Sepulveda, L., Elustondo, D., and Ananias, R. A. (2016). "The development of moisture and strain profiles during predrying of *Eucalyptus nitens*," *Drying Technology* 34(4), 428-436. DOI: 10.1080/07373937.2015.1060490

Svensson, S., Turk, G., and Hozjan, T. (2011). "Predicting moisture state of timber members in a continuously varying climate," *Engineering Structures* 33(11), 3064-3070. DOI: 10.1016/j.engstruct.2011.04.029

Toratti, T., and Svensson, S. (2000). "Mechano-sorptive experiments perpendicular to grain under tensile and compressive loads," *Wood Science & Technology* 34(4), 317-326. DOI: 10.1007/s002260000059

Vaziri, M., Lindgren, O., and Pizzi, A. (2011). "Influence of welding parameters and wood properties on the water absorption in Scots pine joints induced by linear welding," *Journal of Adhesion Science & Technology* 25(15), 1839-1847. DOI: 10.1163/016942410X525731

Virta, J., Koponen, S., and Absetz, I. (2006). "Measurement of swelling stresses in spruce (*Picea abies*) samples," *Building & Environment* 41(8), 1014-1018. DOI: 10.1016/j.buildenv.2005.10.012

Yu, H. Q., Yuan, D., Zhang, X. Y., Fei, B. H., and Liu, H. Z. (2011). "Finite element analysis on the deformation of bamboo-wood composite flooring," *Journal of Building Materials* 14(6), 793-797. DOI: 10.3969/j.issn.1007-9629.2011.06.014

Zhou, H. Z., Zhu, E. C., Fortino, S., and Toratti, T. (2010). "Modelling the hygrothermal stress in curved glulam beams," *Journal of Strain Analysis for Engineering Design* 45(2), 129-140. DOI: 10.1243/03093247jsa563

Zhan, T., Jiang, J., Lu, J., Zhang, Y., and Chang, J. (2018a). "Influence of hygrothermal condition on dynamic viscoelasticity of Chinese fir (*Cunninghamia lanceolata*). Part 1: moisture adsorption," *Holzforschung* 72(7), 567-578. DOI: 10.1515/hf-2017-0129

Zhan, T., Jiang, J., Lu, J., Zhang, Y., and Chang, J. (2018b). "Influence of hygrothermal condition on dynamic viscoelasticity of Chinese fir (*Cunninghamia lanceolata*). Part 2: moisture desorption," *Holzforschung* 72(7), 579-588. DOI: 10.1515/hf-2017-0130

Article submitted: May 31, 2018; Peer review completed: July 31, 2018; Revised version received and accepted: August 6, 2018; Published: August 14, 2018.
DOI: 10.15376/biores.13.4.7395-7403